10-23-2015

High Temperature Proton Exchange Membranes With Enhanced Proton Conductivities At Low Humidity and High Temperature Based On Polymer Blends and Block Copolymers of Poly(1,3-Cyclohexadiene) and Poly(ethylene Glycol)

Shawn Deng
The University of Tennessee, Knoxville

Mohammad K. Hassan
University of Southern Mississippi

Amol Nalawade
University of Southern Mississippi

Kelly A. Perry
Oak Ridge National Laboratory

Karren L. More
Oak Ridge National Laboratory

*Graphical Abstract

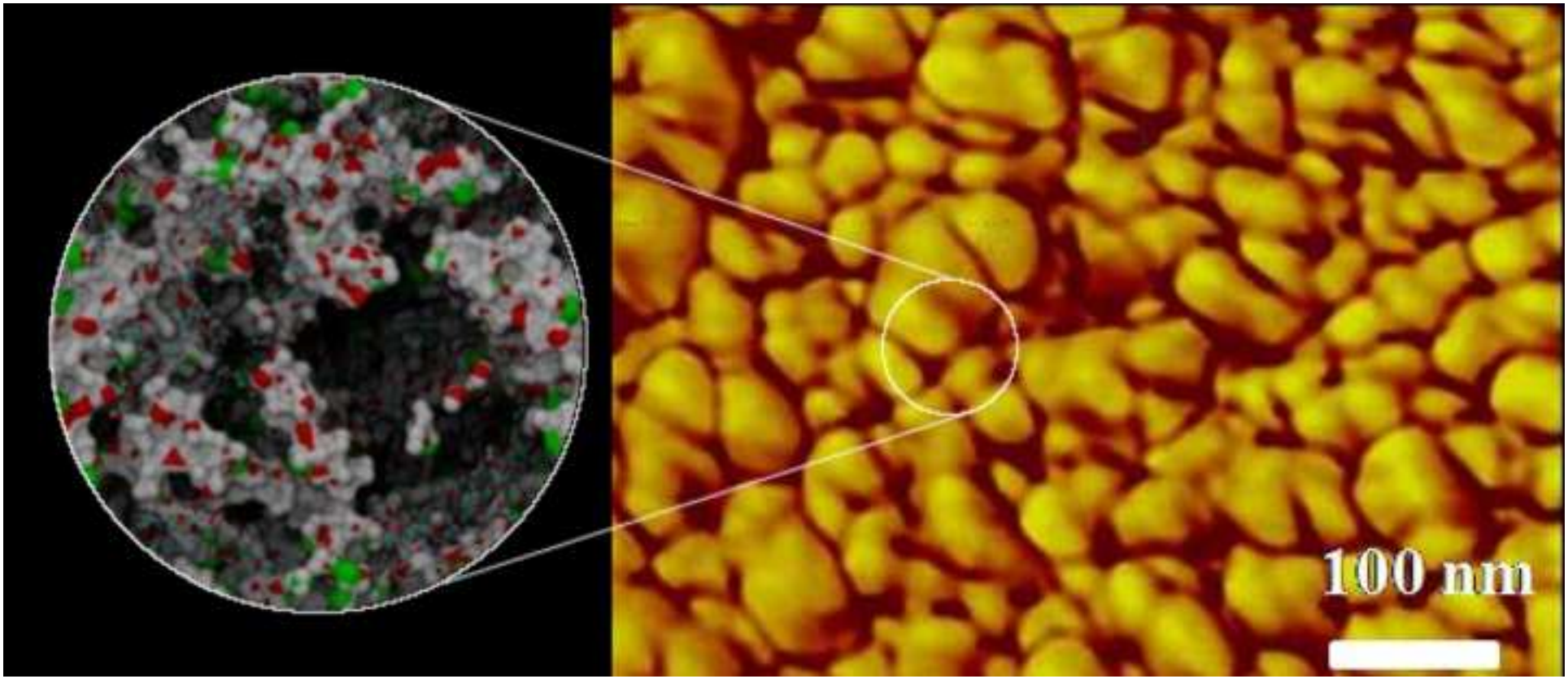

High Temperature Proton Exchange Membranes with Enhanced Proton Conductivities at Low Humidity and High Temperature based on Polymer Blends and Block Copolymers of Poly(1,3-cyclohexadiene) and Poly(ethylene glycol)

By Shawn Deng[a,†], Mohammad K. Hassan[b,‡], Amol Nalawade[b,+], Kelly A. Perry[c], Karren L. More[c], Kenneth A. Mauritz[b], Marshall T. McDonnell[d], David J. Keffer[e,], and Jimmy W. Mays[a,f]*

[a]Department of Chemistry, University of Tennessee, Knoxville, TN 37996, USA

[b]School of Polymers and High Performance Materials, University of Southern Mississippi, Hattiesburg, MS 39406, USA

[c]Materials Science and Technology Division, Oak Ridge National Laboratory, Oak Ridge, TN 37831, USA

[d]Department of Chemical and Biomolecular Engineering, University of Tennessee, Knoxville, TN 37996, USA

[e]Department of Materials Science and Engineering, University of Tennessee, Knoxville, TN 37996, USA

[f]Chemical Sciences Division, Oak Ridge National Laboratory, Oak Ridge, TN 37831, USA

Corresponding Author

*Email: dkeffer@utk.edu

Present Addresses

† Battery Cell Research Group, General Motors China Science Lab, GM (China) Investment Co. Ltd., Shanghai 201206, P. R. China.

‡Center for Advanced Materials, Qatar University, Doha, Qatar.

+Intel Corporation, F11X, Rio Rancho, NM 87124.

KEYWORDS

Proton exchange membrane; poly(ethylene glycol); poly(1,3-cyclohexadiene)

ABSTRACT

Hot (at 120 °C) and dry (20% relative humidity) operating conditions benefit fuel cell designs based on proton exchange membranes (PEMs) and hydrogen due to simplified system design and increasing tolerance to fuel impurities. Presented are preparation, partial characterization, and multi-scale modeling of such PEMs based on cross-linked, sulfonated poly(1,3-cyclohexadiene) (xsPCHD) blends and block copolymers with poly(ethylene glycol) (PEG). These low cost materials have proton conductivities 18 times that of current industry standard Nafion at hot, dry operating conditions. Among the membranes studied, the blend xsPCHD-PEG PEM displayed the highest proton conductivity, which exhibits a morphology with higher connectivity of the hydrophilic domain throughout the membrane. Simulation and modeling provide a molecular level understanding of distribution of PEG within this hydrophilic domain and its relation to proton conductivities. This study demonstrates enhancement of proton conductivity at high temperature and low relative humidity by incorporation of PEG and optimized sulfonation conditions.

1. Introduction

Fuel cells based on proton exchange membranes (PEMs) are considered as viable replacements for traditional power sources, especially internal combustion engines in vehicles.[1] The benchmark PEM remains Nafion, against which other experimental membranes are usually compared. Although Nafion membranes exhibit excellent chemical stability owing to perfluorination, they are expensive and conduct protons poorly at low relative humidity (RH).[2] Transport of protons occurs via a combination of mechanisms: the vehicular (center-of-mass) diffusion mechanism and the structural (proton hopping) diffusion mechanism, also known as the Grotthuss mechanism.[3, 4] In Nafion, proton transport requires a membrane-spanning aqueous domain to facilitate either mechanism across the membrane.[5-9] Thus, fuel cells using Nafion must operate at temperatures lower than 90 °C under atmospheric pressures to prevent dehydration.[10] Also, the low glass transition temperature (Tg) of Nafion promotes physical degradation at fuel cell temperatures owing to mechanical hysteresis that occurs during hydration-dehydration cycling.[11-16]

On the other hand, operating fuel cells at higher temperatures (> 120 °C) and lower RH is attractive for the following reasons: (a) system complexity is reduced by limiting or eliminating the need for water management; (b) the cooling system is simplified; (c) carbon monoxide tolerance is improved; (d) there is possible use of co-generated heat; (e) catalyst amounts are reduced.[10, 17] Therefore, once all factors are considered, there is a need for low cost, high Tg PEMs based upon non-fluorinated materials.[18, 19] High proton conductivity at high temperatures and low RH is critical to the development of a next generation of fuel cells.

Promising high temperature PEMs based on hydrocarbon-polymers having high Tg are largely composed of aromatic polymers as they are chemically and thermally stable.[20-34] Although some aliphatic polymers such as poly(ethylene glycol) (PEG)[35] and poly(ethylene imine) (PEI)[36] are used in acid-base polymer complexes there are few reports of sulfonated aliphatic polymers used as fuel cell membrane materials.[37, 38]

Recently, we reported the first aliphatic proton exchange membrane material based on poly(1,3-cyclohexadiene) (PCHD).[39, 40]Chemical durability of hydrocarbon membranes poses an issue due to the aliphatic hydrogens being susceptible to attack by peroxy and hydroperoxy radicals generated during fuel cell operation.[38, 41]Recognizing that chemical durability is a serious issue, these are considered as limited model systems that nonetheless have a number of variables which can be manipulated to optimize other properties. The chemical and mechanical durability are coupled and a study of this correlation would be a large effort in itself. Ideally, one would optimize in a single effort both functionality, in this case proton conductivity and water distribution, and also chemical and mechanical durability. Realistically, we adhere to a standard approach of demonstrating functionality, through polymer chemistry, to be followed by the use of that knowledge as a framework from which the engineering issues of mechanical stability and lifetime degradation can be investigated. This study does not focus on the chemical and mechanical durability but instead on manipulating a limited number of experimental variables to explore chemical structure and its effects on proton conductivity.

PCHD can be readily incorporated into a range of homopolymer and copolymer structures. The in-chain six-member ring structure of PCHD imparts a much higher Tg (> 100 °C) than that of other polydienes.[42] The double bonds in PCHD can be chemically modified through a host of reactions including hydrogenation,[43] aromatization,[44] sulfonation,[45] and even

fluorination[46] which allow for tuning key performance properties such as proton conductivity, mechanical properties, morphology, thermal stability and cost. PEMs based on PCHD are thermally stable and of potentially low cost since the monomer 1,3-cyclohexadiene is easy to synthesize and can be inexpensive if produced commercially.

In this work, PCHD-based membranes were synthesized as shown in Scheme 1, Scheme 2, and Scheme 3. The polymers were first crosslinked (x) to give membranes xPCHD and then sulfonated (s) to produce fuel cell membranes xsPCHD. The xsPCHD homopolymer, xsPCHD-PEG polymer blend, and xsPCHD-PEG diblock copolymer membranes were characterized and evaluated within the context of high temperature fuel cell applications. The ultimate goal of this work is to develop low cost, high temperature, low humidity PEMs that can minimize the need for water management in automotive fuel cells.

Scheme 1. Synthesis Route of xsPCHD Homopolymer PEMs.

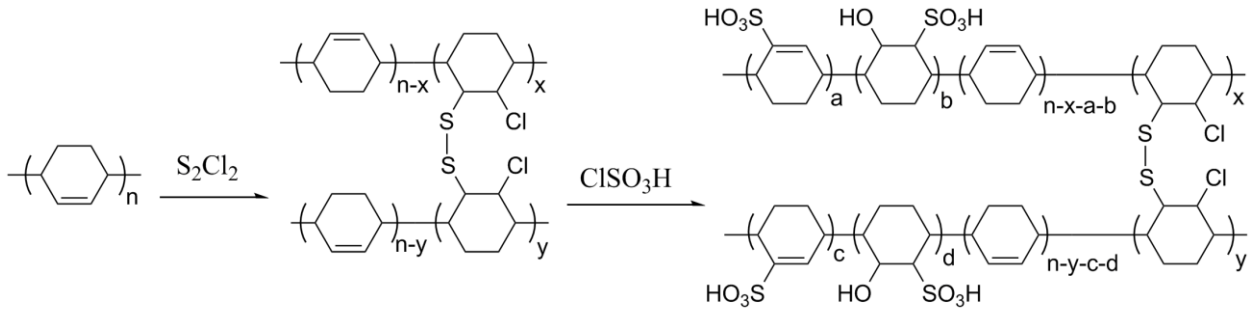

PCHD **xPCHD** **xsPCHD homopolymer**

Scheme 2. Synthesis Route of xsPCHD-PEG Blend PEMs.

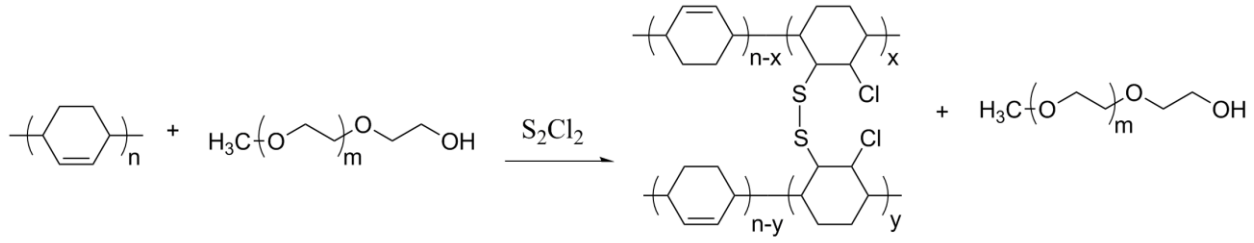

Polymer blends of PCHD and PEG **xPCHD-PEG blend**

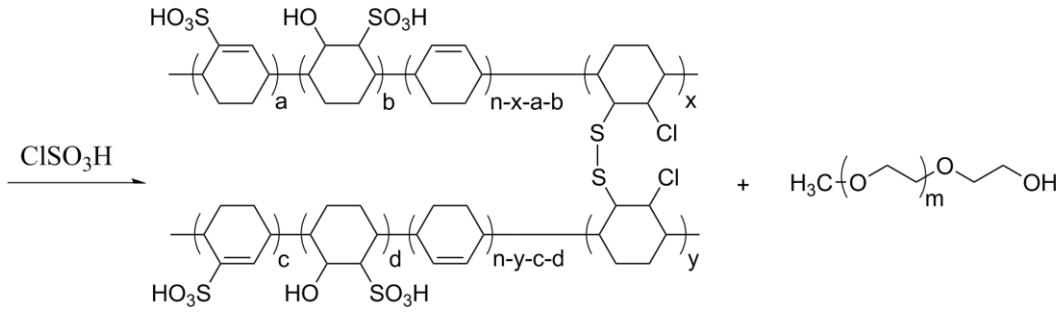

xsPCHD-PEG blend

Scheme 3. Synthesis Route of xsPCHD-PEG Block Copolymer PEMs.

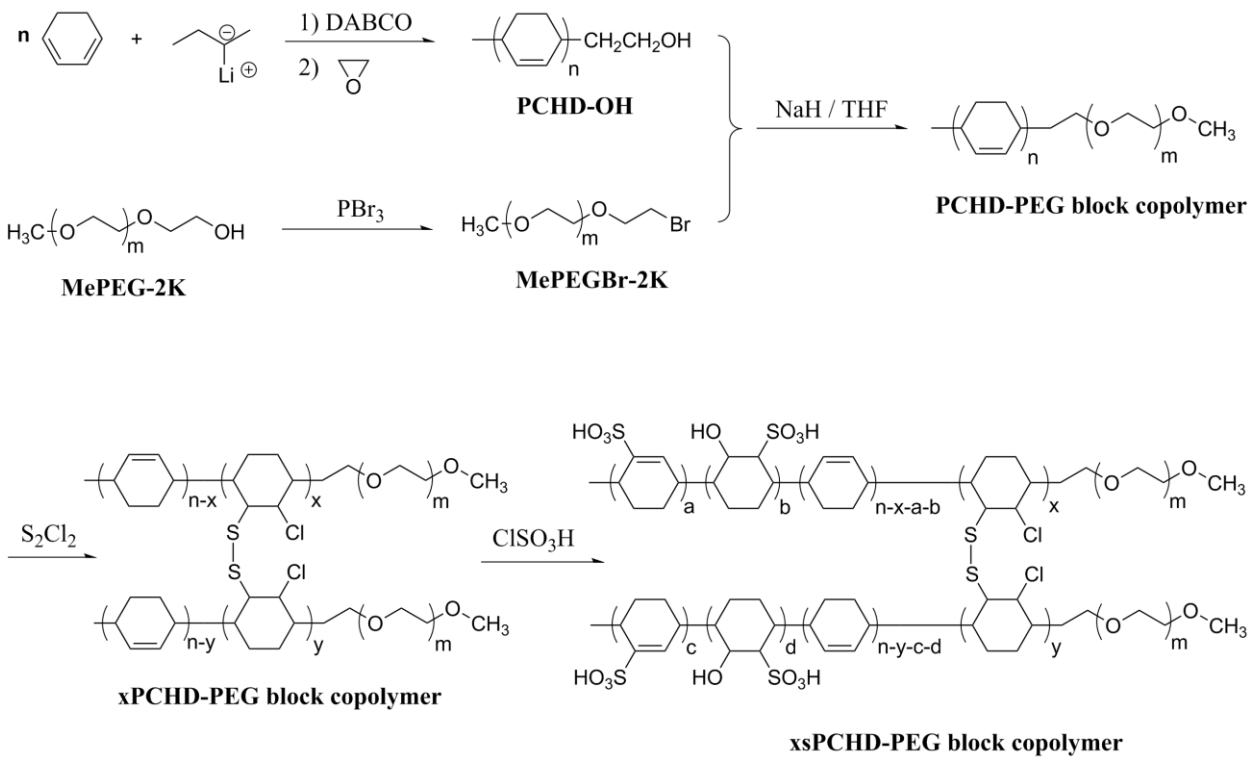

2. Experimental Section

2.1Materials

Benzene (Fisher, 99%), tetrahydrofuran (THF), 1,3-cyclohexadiene, and 1,4-diazabicyclo-[2.2.2]octane (DABCO, Aldrich, 98%) were purified as previously reported.[47] Poly(ethylene glycol) methyl ether (M_n = 750 and 2000) were dried at 60 °C under vacuum for 24 h. Bromide-terminated poly(ethylene glycol) methyl ether (MePEGBr-2K) having M_n of 2,000 g mol^{-1} was synthesized as previously reported.[48]Chlorosulfonic acid ($ClSO_3H$, 98%, Fluka), *sec*-Butyllithium (Aldrich, 1.4 M in cyclohexane), sulfur monochloride (S_2Cl_2, 99.9%, Aldrich), 1,2-dichloroethane (99.8%, Aldrich), 2,6-di-tert-butyl-4-methylphenol (butylated hydroxytoluene,

BHT, Aldrich, 99%), cesium iodide (CsI, 99.9%, Aldrich), and all other solvents were used as received

*2.2Synthesis of polymers***.**

2.2.1Hydroxyl-terminated poly(1,3-cyclohexadiene) (PCHD-OH) synthesis. All polymerizations were carried out under high vacuum using custom-made glass reactors. In a typical polymerization experiment, about 250 mL of purified benzene was distilled into a reactor with all the purified reagents attached via break-seals. The reactor was removed from the vacuum line after evacuation. About 4.0 mL of home-made *sec*-BuLi (0.40 M in hexane, 1.6 mmol) and 0.5 g of DABCO (4.5 mmol) in benzene (10 mL) were introduced into the reactor. After stirring for 5 min. at room temperature, 35 mL of 1,3-cyclohexadiene (29.5 g, 0.37 mol) was added. After about 6 h, about 1.0 mL of ethylene oxide was added to end-cap the living polymer. The reaction was allowed to continue overnight and terminated with acidic methanol. The polymer solution was poured into a large excess of methanol. The precipitated polymer was collected by filtration and dried under vacuum (27.0 g, ~ 90% yield). The obtained polymer was either used to prepare diblock copolymer within one week or sealed in ampoules to prevent oxidative degradation. GPC: M_n 19.0 Kg mol^{-1}, PDI 1.18. ^{1}H NMR spectrum (see Supplementary Data S.1SupplementaryFig.1).

2.2.2Poly(1,3-cyclohexadiene) (PCHD) synthesis. Two batches of homopolymers PCHD-1 and PCHD-2 were synthesized by following the same procedure as described above. However, ethylene oxide was not used to end-cap the living polymer. Commercially available *sec*-BuLi (Aldrich, 1.4 M in cyclohexane) instead of home-made *sec*-BuLi was used as the initiator. During precipitation, BHT was added in methanol to prevent oxidative degradation of PCHD.

PCHD-1 was used for homopolymer membranes while PCHD-2 for polymer blends membranes. GPC of PCHD-1: M_n19.0 Kg mol^{-1}, PDI 1.34. GPCof PCHD-2: M_n 25.5 Kg mol^{-1}, PDI 1.53.

2.2.3 Poly(1,3-cyclohexadiene-b-ethylene oxide) diblock copolymer PCHD-PEG (~ 9.5 wt% PEG) synthesis. Under argon, PCHD-OH (5.0 g, ~ 0.26 mmol of terminal hydroxyl groups), MePEGBr-2K (0.8 g, 0.40 mmol of terminal bromide groups), and CsI (~ 100 mg) were added into 300 mL of anhydrous THF. About 200 mg of NaH (60% dispersion in mineral oil) was added in small portions. The mixture was stirred overnight at room temperature and poured into water. The crude product was collected by filtration, dried under vacuum, and then dissolved in toluene. The polymer solution was poured into a large excess of methanol with BHT to prevent oxidative degradation. The precipitated polymer was collected by filtration and dried under vacuum. About 4.2 g of white solid was obtained (~ 75% yield). GPC: M_n 21.1 Kg mol^{-1}, PDI 1.15. ^{1}H NMR spectrum (see Supplementary Data S.1SupplementaryFig.2).

2.3Membrane Casting.

2.3.1Crosslinked homopolymer (xPCHD) and diblock copolymer (xPCHD-PEG) membrane casting. All membranes were solution cast in air. The molar ratio of S_2Cl_2 to double bonds in PCHD varied from 20% to 50%. The diameter of membranes ranged from 50 to 150 mm and the PCHD weighed from 0.2 to 0.5 g. In a typical membrane casting experiment, 0.10 g of S_2Cl_2 (0.74 mmol) in toluene (1.0 mL) was added drop-wise into 0.25 g of PCHD-1 (homopolymer, M_n 19.0 Kg mol-1, PDI 1.34) or PCHD-PEG (diblock copolymer, M_n 21.1 Kg mol-1, PDI 1.15, ~ 9.5 wt% PEG) in toluene (4.0 mL). After addition, the reaction mixture was stirred at room temperature for ~1 h and then poured into a Fisher brand Low-Form PTFE dish (100 mm in diameter). The solvent was slowly evaporated overnight in a hood. The membranes were peeled

off carefully with a spatula, washed twice with hexane, and further dried under vacuum overnight while keeping samples pressed between desiccator plates. The thicknesses of the membranes were easily controlled by varying the amounts of polymer or the diameter of the PTFE dish.

2.3.2Crosslinked polymer blend (xPCHD-PEG blend) membrane casting. The polymer blend membranes were prepared by following the same procedure as described above, but a mixture of PCHD-2 (0.25 g, M_n 25.5 Kg mol-1, PDI 1.53) and MePEG (M_n = 750, 28.0 mg) was used. Moreover, more solvent (8.0 mL of toluene) was used to reduce phase separation between PCHD and PEG. The optimized polymer blends contained 10 wt% PEG. Varying amounts of PEG were previously incorporated in the xPCHD/PEG membranes but molecular weight, sulfonation conditions, and pre-treatment proved to be stronger factors for optimizing proton conductivities for the membranes. This is shown in Supplementary Data S.2 Supplementary Table 1where membranes with similar (9.1 wt% PEG) and different (16.7 wt% PEG) PEG compositionbut with higher molecular weight PEGare shown with much lower conductivities compared to those of Fig. 1 with membranes of 10 wt% PEG and lower molecular weight (750 g mol-1). PEG composition does not seem to be the dominant factor in optimizing proton conductivity compared to other factors such as molecular weight of PEG.

2.4Proton Exchange Membranes (PEMs): Sulfonation of Crosslinked Membranes.

*2.4.1 Crosslinked sulfonated homopolymer (xsPCHD) membranes.*All sulfonation experiments were performed under N_2 atmosphere to reduce the effect of moisture. The molar ratio of $ClSO_3H$ to double bonds in xPCHD (calculated before crosslinking) ranged from 1.4 to 7.0. The degree of sulfonation as determined by elemental analysis varied from 20 mol% to 90%. In a

typical sulfonation experiment, about 200 mL of anhydrous 1,2-dichloroethane was added onto a crosslinked membrane xPCHD (~ 0.25 g, 3.1 mmol double bond units) placed above a desiccator plate (diameter:140 mm) in a 1.0 L cylindrical reactor. A solution of $ClSO_3H$ (2.5 g, 21.5 mmol, 6.88 molar equivalent) in 1,2-dichloroethane (~ 10 mL) was added drop-wise, and the reaction mixture was then refluxed for 2 h. The solution was cooled to room temperature. Then the membrane was taken out, washed with methylene chloride and further immersed in NaOH aqueous solution (10 wt%) for about 30 min. It was washed with water, immersed in dilute hydrochloric acid (5 wt% HCl) for 15 min., and washed with plenty of water. Finally, the membrane was dried overnight under vacuum at room temperature while pressed between two desiccator plates.

*2.4.2Crosslinked sulfonated diblock copolymer (xsPCHD-PEG block copolymer) membranes.*Under N_2, about 200 mL of anhydrous 1,2-dichloroethane was added onto a crosslinked membrane xPCHD-PEG (~ 0.25 g, ~ 9.5 wt% PEG, 2.81 mmol double bond units) placed above a desiccator plate (diameter:140 mm) in a 1.0 L cylindrical reactor. A solution of $ClSO_3H$ (2.2 g, 18.9 mmol, 6.73 molar equivalent) in 1,2-dichloroethane (~ 10 mL) was added drop-wise, and the reaction mixture was stirred at room temperature for 1 h and then heated with refluxing for 1 h. The solution was cooled to room temperature, and the membrane was then washed with methylene chloride and further immersed in 1,4-dioxane with 5 wt% water for about 30 min. Finally, the membrane was dried overnight under vacuum at room temperature while pressed between two desiccator plates.

*2.4.3Crosslinked sulfonated polymer blend (xsPCHD-PEG blend) membranes.*The polymer blend membrane xsPCHD-PEG blend was prepared by following the same procedure as that for

xsPCHD-PEG block copolymer, but only 2.0 g of $ClSO_3H$ (2.2 g, 17.2 mmol, 6.12 molar equivalent) was used.

2.5Characterization

Gel permeation chromatography (PL-GPC 120) was used to determine molecular weights and polydispersity indices (M_w/ M_n) of the polymer samples with respect to polystyrene standards (PSS, Germany). The unit was equipped with RI, light scattering 15 and 90° (Precision Detectors 2040, λ=685 nm, 30mW) and differential viscometer (Viscotek 220) detectors. ^1H NMR spectra were recorded on a Varian 300 MHz (Oxford) instrument. The polymer concentration of the sample was around 5 wt%. Elemental analysis services were provided by Galbraith Laboratory Inc. (Knoxville, TN).

2.6 Water uptake

The amount of membrane equilibrium water vapor sorption vs. external relative humidity (RH) was determined at 80 °C (a common fuel cell operating temperature) by using a Q5000SA TA instrument. De-sorption isotherms were determined by hanging samples on a weighing balance (accuracy ≤ ±0.1%) that was placed in a temperature and humidity-controlled chamber. Isothermal water content vs. RH curves were generated while decreasing RH from 90% to 0% in 10% increments.

2.7 Membrane in-plane proton conductivity

Membrane in-plane proton conductivity vs. RH at 120 °C was determined using a BekkTech (BT-512) four-point probe conductivity test system. The sample dimensions were 4.2 mm in length and 5.4 mm in width. Samples were held in place by tightening a clamp. The membrane

was equilibrated at each RH step for 1 h. A back-pressure of 230 kPa absolute was used during the measurements.

2.8 Atomic force microscopy

Atomic force microscopy (AFM) was performed using a Digital Dimension 3000 Nanoscope IIIa instrument. Tapping/phase mode interrogates morphology on the basis of local viscoelastic properties, i.e., hard vs. soft regions. A silicon probe with nominal force constant of 40 N/m and resonance frequency of 275 kHz was used for tapping. Bulk morphologies of samples, microtomed using a glass knife, were studied on 1 μm x 1 μm scan size areas at a scan rate of 0.5 Hz. Tapping mode was used to preserve the surface topography of the sample so that results were reproducible. Multiple areas were imaged.

2.9 TEM / SEM imagery

Microstructural characterization also included imaging of freeze-fractured cross-sections in a Hitachi S4800 SEM and of cryo-microtomed thin cross-sections in a Hitachi HF3300 TEM.

2.10 Thermogravimetric analysis (TGA)

Thermal stability of all membranes was analyzed using a Thermogravimetric Analyzer TA Q50 (TGA). Sample sizes were under 10 mg and heated under 25 ml/min of nitrogen from 30 °C to 800 °C at the heating rate of 10 °C/min.

3.Results and Discussion.

3.1 Crosslinking, sulfonation and PEG incorporation for xsPCHD/PEG membranes

PEG was chosen as a component because of its potential to retain water and thus increase proton conductivity at low humidity.[48] PCHD homopolymers, block copolymers containing about 9.5 wt% PEG, and polymer blends (~ 10 wt% PEG) were slightly crosslinked (2 ~ 5 mol.%) with sulfur monochloride (S_2Cl_2) in toluene and then solution-cast to form free-standing films. Without crosslinking, the solution-cast films are too brittle to be peeled off the casting substrate. Crosslinking not only makes solution-cast films considerably more flexible but locks in the morphology of PEMs (after sulfonation). Therefore, crosslinking is essential for preparation of these PEMs. Sulfonation is also critical in the control of PEM properties, not just proton conductivity but mechanical integrity as well. In general, higher degrees of sulfonation lead to better proton conductivity although too high a degree results in a loss of mechanical integrity. The highest degree of sulfonation beyond which the homopolymer PEMs (xsPCHD) becomes mechanically weak is 50 mol %. On the other hand, the xsPCHD-PEG diblock copolymer can reach 80% sulfonation and xsPCHD-PEG blends can reach 90% sulfonation. Similar to sulfonation of polysulfones, [49-51]fragmentation of the polymer backbone can make PEMs mechanically weak. For xsPCHD, although a large excess of chlorosulfonic acid $ClSO_3H$ (6.88 equivalents) and high temperature (~ 80 °C) were used, only 50% sulfonation was obtained. Therefore, the diffusion of $ClSO_3H$ into membranes was not efficient, leading to quite serious fragmentation. Low Tg polymer PEG (M_n: 2,000 g mol^{-1}) in xsPCHD-PEG block copolymer facilitates the diffusion of $ClSO_3H$ so that less fragmentation and higher degree of sulfonation were obtained. PEG of lower molecular weight (M_n: 750 g mol-1) in a xsPCHD-PEG blend can partially leach out during sulfonation, which leads to more efficient diffusion of $ClSO_3H$ and lesser fragmentation as compared with a xsPCHD-PEG block copolymer. This leaching of PEG

only decreases the overall membrane PEG composition by ~2 wt% and is not considered to be significant enough to effect the overall composition or membrane morphology.

Sulfonation chemistry, despite its commercial utility, remains complex and is not well understood because olefin sulfonation can produce a myriad of reaction products depending on olefin structures, sulfonating reagent conditions, and work-up procedures.[52, 53]Different reaction temperatures and work-up procedures used gave rise to different sulfonation products and thus different microstructures in these PEMs.[40, 54] The differences in degree of sulfonation and microstructures among the xsPCHD, xsPCHD-PEG blend and xsPCHD-PEG block copolymer are the major attributors to the differences in PEM properties such as water uptake, proton conductivity and morphology.

3.2 Membrane water uptake

Water vapor pressure isotherms at 80 °C are shown in Fig. 1. Curves for the average number of moles of water per mole of sulfonic acid groups (λ) vs. RH show that the water uptakes of the homopolymer, blend and block copolymer materials are significantly higher than that of Nafion 112 over the higher RH range with the blend showing the greatest hydration.

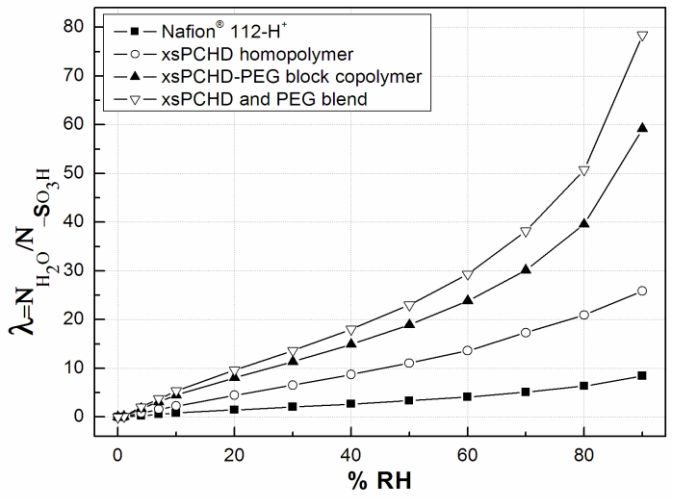

Fig. 1. Water uptake in PEMs at 80 °C.λ vs. RH for Nafion 112 (■), xsPCHD homopolymer(○), xsPCHD-PEG block copolymer (▲), and an xsPCHD-PEG blend (▽).

For example, at 50% RH xsPCHD membranes have 10-20 times the water uptake of Nafion. The greater hydration capacity of the copolymer and blend is attributed to the presence of hydrophilic, conformationally-flexible PEG components. At 50% RH, the xsPCHD-PEG copolymer and xsPCHD-PEG blend incorporate ~ 5 times the number of water molecules per acid group than Nafion. Given these large λ values, it is reasonable to assume that the state of water in the xsPCHD systems is more liquid-like for RH > 20% because there are more than enough water molecules to form hydration shells around the SO3- groups on average.[55] This is important for PEMs that are dependent on water-based proton conduction even at low RH.

3.3. Membrane proton conductivity

Corresponding proton conductivity vs. RH curves for Nafion 112 and for all the xsPCHD-based membranes are displayed in Fig. 2. The conductivities of all the xsPCHD based samples at 120 °C for low (20%), medium (50%) and high (80%) RH values are listed in Supplementary Data

S.2 Supplementary Table 1. The xsPCHD homopolymer has higher conductivity than Nafion 112 at RH > 80% but decreases sharply as RH decreases. Both block copolymer and blend PEMs have higher proton conductivity than Nafion over the entire RH range (20% to 100%). At RH = 50% the conductivities of the block copolymer and blend are, respectively, 4 and 9 times that of Nafion. At low (20%) RH, the conductivities of the block copolymer and blend PEMs are, respectively, as high as 5 and 18 times that of Nafion. Both samples exceed the DOE target proton conductivity for 2015 indicated in Fig. 2 (> 0.1 S cm-1 at 50 % RH and 120 °C).[56] As compared with the xsPCHD homopolymer, the higher conductivities of xsPCHD-based copolymer and blend materials at low RH are related to their higher water uptake, as seen in Fig. 1, due to the hydrophilicity of the PEG component.

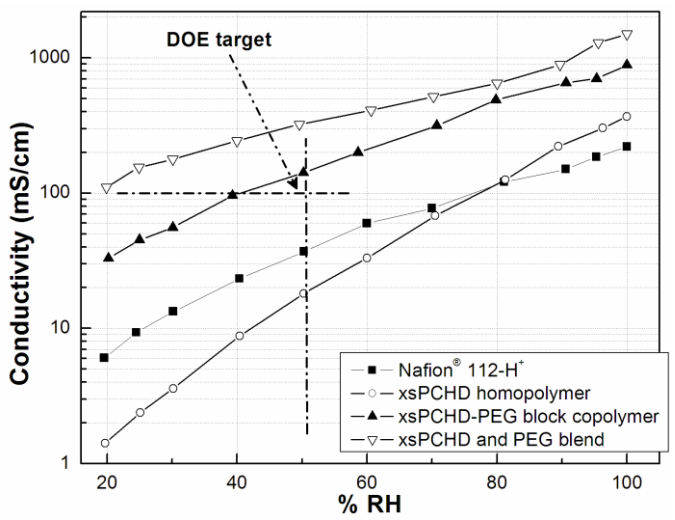

Fig. 2. Proton conductivity vs. RH for Nafion (■), xsPCHD homopolymer (○), xsPCHD-PEG block copolymer (▲) and xsPCHD-PEG blend (▽) at 120 °C.

There are several potential mechanisms for the enhanced proton conductivity observed in the block copolymer and blend PEMs. First, the presence of the hydrophilic PEG component serves

to enhance water retention. In many PEMs, the mobility of both water and charge are highly correlated with the amount of water in the membrane. This additional water can potentially impact proton conductivity in more than one way. At a mesoscopic level, higher water content can result in the presence of a membrane-spanning aqueous domain providing a continuous path for proton transport per percolation theory.[7-9] At the atomic level, higher water content promotes dissociation of excess protons from the sulfonate anions and enhances both the local vehicular and structural components of proton transport.[57] The influence of PEG on the conductivity mechanism is not immediately clear. Additional discussion of the effects of PEG is given later.

3.4 Membrane morphology: Atomic force microscopy imagery

The comparatively high proton conductivity at high temperature and low RH reflects well-formed networks of contiguous aqueous domains at higher water content and phase-separated morphologies as will be discussed in the atomic force microscopy (AFM) results presented below. Tapping mode/phase AFM images of these xsPCHD-based materials shown in Fig. 3 reveal phase separated morphologies with features less than 10 nm in size. McGrath et al[58] observed similar surface morphologies for their sulfonated copolymer materials with hydrocarbon backbones. The bright regions are assigned to crosslinked hydrophobic non-ionic domains while the dark regions are assigned to hydrophilic sulfonated domains. This assignment is largely based on the higher fraction of hydrophobic vs. hydrophilic chemical groups in the primary polymer structure. This contrast is due to the phases having different local viscoelastic properties. A PEG domain will be 'softer' than an xsPCHD domain. For the copolymer and the blend, the hydrophilic PEG components result in larger and more contiguous darker regions. Increased connectivity of hydrophilic domains offers more efficient proton transport pathways

which contributes to the high conductivities observed for these membranes vs. that of the xsPCHD homopolymer, as shown in Fig. 2. In the case of the block copolymer, the PEG block molecular weight is 2,000 g mol-1 vs. 750 g mol-1 for the blend's unbound PEG molecules. From these images, it appears that the aqueous domains in the blend are smaller than those in the copolymer.

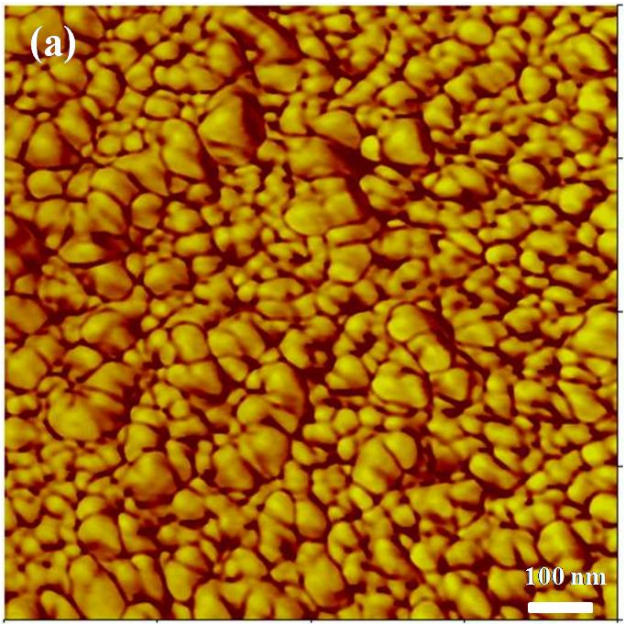

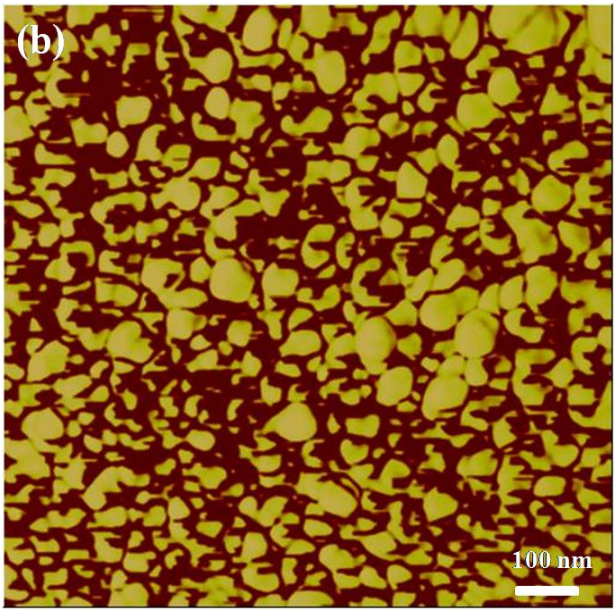

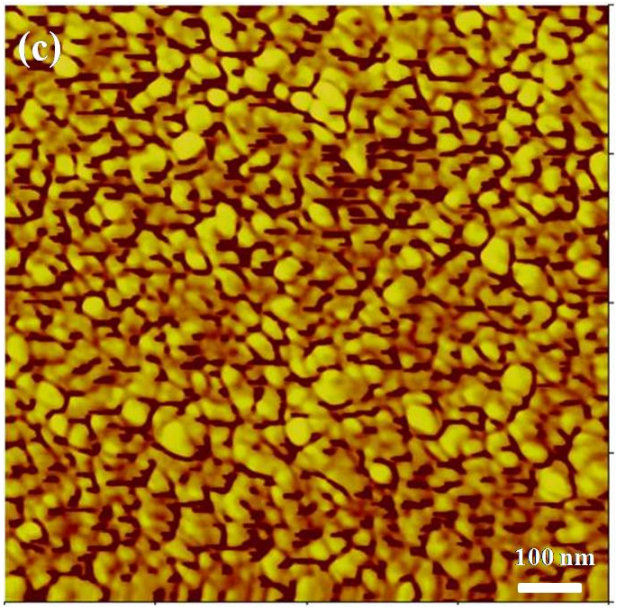

Fig. 3. Tapping mode AFM phase images. (a) xsPCHD homopolymer, (b) xsPCHD-PEG block copolymer and (c) xsPCHD-PEG blend.

Microstructural characterization of these materials was also conducted using scanning electron microscopy (SEM) and transmission electron microscopy (TEM). SEM images of freeze-fractured cross section morphology are shown in Supplementary Data S.3 Supplementary Figure 3. All three membrane types exhibited microstructural heterogeneitywith prominent features up to 200μm in size.

3.5 Modeling and simulation of membranes

3.5.1 Modeling and simulation: Structure and morphology

A multi-scale modelling effort of a similar polymer chemistry, involving atomistic molecular dynamics (MD), coarse-grained molecular dynamics (CGMD),[59-61] confined random walk (CRW) simulations[61-63] and percolation theory,[61-63] has been performed to describe the xsPCHD and PEG melts[59, 60] and hydrated membranes of the homopolymer,[61-

63]copolymer[62], and blend[62] to further investigate structure and transport.[59-63] The polymer chemistry simulated consists of the same xsPCHD backbone with different PEG linking in the copolymer. Also, the simulated PEG polymer terminates in hydroxyl groups rather than ether groups. This minor difference in polymer chemistry still provides a meaningful understanding of the water distribution in the membrane consistent with the AFM imagery, providing molecular insight into the morphology, PEG distribution, and transport across the membrane, to be discussed later.

To investigate the membrane morphologies over different length scales, appropriate modeling and simulation techniques are chosen to extract relevant information for the given scale of interest. On the smallest scale, the fully atomistic MD simulations give correlations between atomic pairs like those between polymer monomer atoms and the molecules of the aqueous domain, such as those shown in Fig. 5. On a larger atomic length scale, CGMD simulations of the xsPCHD homopolymer lose atomic-level resolution yet are able to show the aqueous channel diameter to be on the order of 10 nm, shown in Fig. 4. This aqueous channel diameter is comparable with the aqueous domain sizes in the phase morphology seen in the AFM images in Fig. 3 and discussed previously in other work.[61]On the largest length scale, yet lowest resolution,CRW simulations[62]of the mesoscale suggestthat the water cluster size radius in the blend (12.2 Å) is smaller than that in the homopolymer (15.8 Å) and significantly smaller than that for copolymer (24.1 Å).

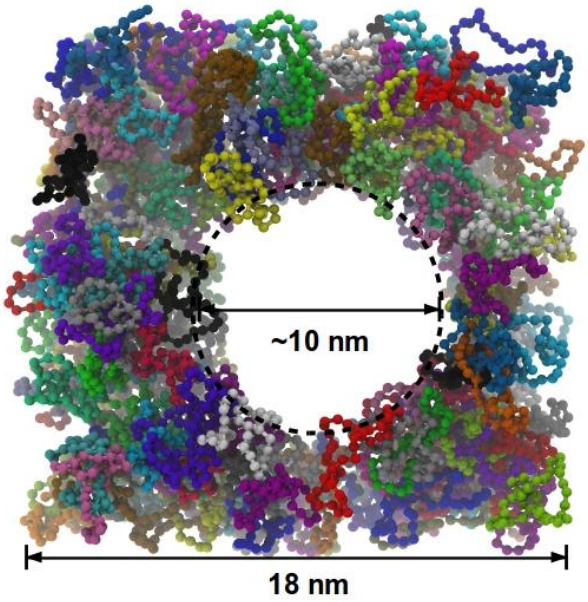

Fig.4 Simulation image of hydrated xsPCHD membrane with coarse-grained potentials for hydrated polymer beads using the NPT ensemble. The state point was set at 1 atm, 80 °C and λ = 10. Due to the hydrating species being implicitly incorporated into the coarse-grained potential interaction between coarse-grained polymer beads, only the polymer chains are explicitly simulated (colored by chain) and shown with the nanopore of ~10 nm being the aqueous channel formation.

Pair correlation functions from fully atomistic MD simulations of water, hydronium ions (proton carriers), and PEG monomer species for the xsPCHD-PEG copolymer and blend membranes highlight key differences in structure and distribution of PEG for both membranes.[62] The hydroxyl end groups of PEG have stronger correlation with hydronium ions in the copolymer than in the blend, while the PEG backbone shows stronger correlation with the hydronium in the blend than in the copolymer, shown in Fig.5 (Simulation images produced using Visual Molecular Dynamics visualization software[64]). The water shows an overall stronger

correlation to the hydroxyl groups and backbone of PEG for the blend compared to the copolymer. Fig.5 gives visual insight from simulation images of the xsPCHD-PEG copolymer and blend where only the water, hydronium, and PEG are visible. The water and hydronium create the aqueous domain surface to highlight the larger water cluster size in the copolymer, the higher water dispersion in the blend, and the differences of PEG distribution between both. The key differences between the copolymer and blend are the PEG in the copolymer is located at the interface of the polymer domain and aqueous domain, tethered to the polymer domain and extending into the aqueous domain, aggregating water to create larger clusters. The PEG chains in the blend are located entirely in the aqueous domain and structure water molecules along their lengths and evenly distribute the water in the channel so it is more highly dispersed throughout the membrane. This observation is supported by the pair correlation function data and simulation images from atomistic MD simulations in Fig.5, the CGMD simulation image of the aqueous channel in Fig. 4, the water cluster sizes from the CRW simulations, the visible differences in aqueous domain sizes in the AFM imagery, and further validated by impacts on water diffusion, to be discussed below.

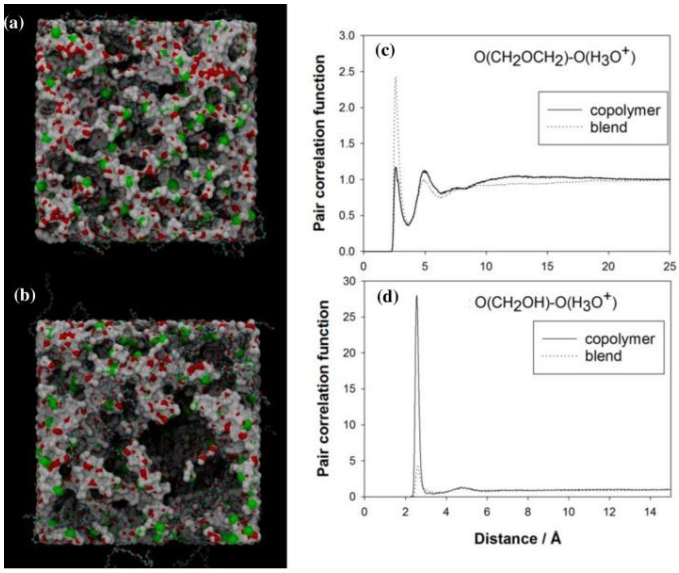

Fig.5 Atomistic simulation images of PEG within the hydrophilic domains of the membranes for xsPCHD-PEG blend (a) and block copolymer (b) and pair correlation functions of hydronium ion with ether of PEG (c) and with hydroxyl of PEG (d) at 80 °C, and $\lambda = 10$. In the simulation images, (a) and (b), only the water, hydronium, and PEG are shown (xsPCHD backbone of the hydrophobic domain was rendered invisible). The water and hydronium [oxygen of water (red), oxygen of hydronium (green) and hydrogen (white)] are represented by the aqueous domain surface while the PEG chains are represented as beads [carbon (blue), oxygen (red) and hydrogen (white)]. The pair correlation functions, (c) and (d), show the correlation of oxygen in hydronium to the oxygen along the backbone of PEG polymers (top right) and the terminal hydroxyl groups of PEG (bottom right).

3.5.2 Modeling and simulation: Transport

The transport of both water and protons is affected due to the incorporation of PEG in the aqueous channels. PEG has been shown experimentally to slow water diffusion[65] and the same effect is observed in our simulation work shown in SupplementaryData S.4

SupplementaryTable 2. In the blend, the PEG additive in the aqueous domain decreases the water mobility and also causes greater tortuosity for water diffusion through the highly dispersed channels. The same effect is observed for the vehicular component of proton transport due to its strong coupling to water transport. Experimentally, we observe that the presence of PEG enhances proton transport. Since the simulations show that the vehicular component is decreased, there are two potential explanations. First, the simulations, limited to a dimension of 8 nm, may not capture a larger scale organization of the aqueous domain. Second, the presence of PEG may actually enhance structural diffusion, which was not modeled in the classical MD simulations. As suggested by Ritchie et al,[48] PEG may facilitate structural diffusion. This suggests the latter explanation as a likely candidate.

Structural diffusion contributions can be incorporated indirectly via percolation theory, which has shown to work well for systems with strong correlation between water and proton transport (Nafion, short-side chain perfluorosulfonic acid based PEMs,[9] and xsPCHD homopolymer membranes[61]). While this approach works well for the homopolymer, it fails for the xsPCHD-PEG copolymer and blend membranes, suggesting that the presence of PEG decouples the water transport from the charge transport. Currently, computational efforts to explicitly evaluate the structural diffusion mechanism in xsPCHD-PEG membranes are underway.

Other research with PEMs based on modified PEG blends has been reported. Both sulfonated and unsulfonated PEG-PEA poly(ethylene glycol) phenyl ether acrylate have been blended with PEGDA poly(ethylene glycol) diacrylate, where PEGDA acts as a crosslinker, improving the mechanical stability of the network.[66] Yet, these PEMs showed lower proton conductivity than Nafion due to a lack of nanoscale segregation of the polymer and aqueous domains. We

believe that the unique segregation behavior and distribution of PEG in the xsPCHD-PEG blend account for the high conductivity.

3.6 Thermogravimetric analysis (TGA)

Unlike Nafion these PEMs based on PCHD are thermally stable up to 150 °C as confirmed by thermogravimetric analysis (TGA) in Fig.6. TGA studies were performed to determine thermal stability in a N_2 (non-oxidative) atmosphere. Fig.6 shows mass loss vs. temperature up to 800 °C. Multi-step degradation is observed for all samples. The first step involves mass loss from the initial temperature up to 200 °C for the homopolymer, and up to 150 °C for the copolymer and blend. Percent weight losses during this step are 8, 15 and 22 wt%, respectively, for the homopolymer, copolymer and blend. This initial weight loss is due to loss of sorbed water. The increasing order in weight loss is similar to that of the membrane hydration capacity, as seen in the water vapor pressure isotherms in Fig. 1.

Williamson et al.[67] observed initial degradation with a weight loss of ~ 12% for PCHD at around 100 °C. Similarly, Natori et al.[68]reported a weight loss of 13 wt% for their PCHD materials in the same temperature range. Since their PCHDs were not sulfonated, which avoids any moisture uptake by membranes, the initial weight loss was attributed to de-polymerization. In our results, the onset of degradation shifted to 150 °C, which may be due to the fact that our xsPCHD materials are cross-linked and sulfonated, which enhances their thermal stability. Thus, for xsPCHD homopolymer, a weight loss of 14 wt% occurs between 150 °C and 300 °C followed by another loss (~ 13 wt%) between 310 °C to 390 °C and a loss of 7 wt% between 400 °C and 530 °C. There is no clear demarcation between these degradation steps. It seems feasible that at 150 °C there is de-polymerization until a more thermally stable end group was achieved,

which then showed a weight loss at 310 °C and 400 °C.[67, 68] In case of the copolymer and blends, the degradation profiles are similar, but with much higher weight loss in the temperature range of 150 °C to 400 °C (~ 40 wt%) as compared to that of xsPCHD homopolymer (~ 26 wt%). This could be due to degradation of PEG in this temperature range.[69]

All membranes showed appreciable amounts of char residue (35 ~ 60% of original mass) at temperatures as high as 800 °C. Natori et al[68] reported that the weight residue for polyphenylene (i.e., completely dehydrogenated PCHD) was between 60 ~ 70 wt% at 800 °C. It thus appears that de-sulfonation could lead to the formation of polyphenylene, although additional studies are required. The multi-step degradation process observed by TGA for xsPCHD-based materials reflects the complexity of these chemical structures, which include SO_3H groups, cross-links and chemical heterogeneity along the backbone. No major weight loss occurs up to ~200 °C for the xsPCHD homopolymer, nor for the copolymer and blend systems up to 150 °C. While the temperatures reached in these tests are above fuel cell operating temperatures, the degradation temperatures reflect material bonding cohesion that is related to membrane durability. The thermal stability at high temperatures affected by this synthetic route is worthy of consideration for membranes in high temperature fuel cells.

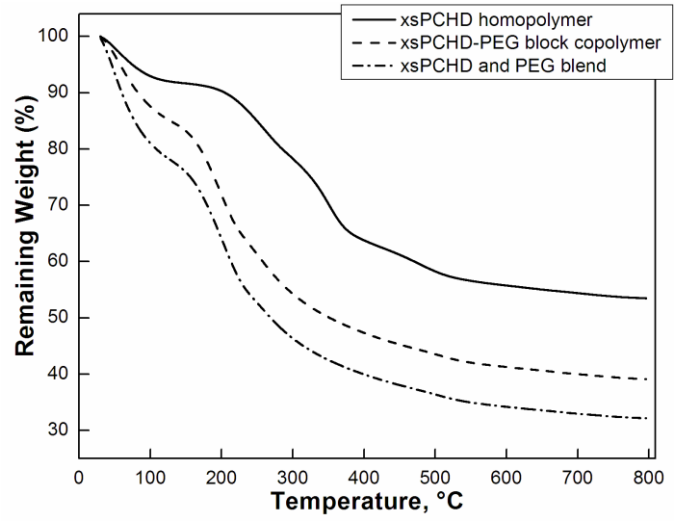

Fig.6. Thermogravimetric analysis thermograms for xsPCHD homopolymer, xsPCHD-PEG copolymer and xsPCHD blend with PEG.

3.8 Future work

Further work should address performance and durability testing of the membranes in membrane electrode assemblies as well as crossover gas permeability testing. The chemical stability can be evaluated by analyzing membranes degraded via accelerated stress tests such as the Fenton's reagent test as well as open circuit voltage testing with broadband dielectric spectroscopy.[70] This analysis could also give insight into degradation mechanisms to help address chemical durability issues. Gas crossover, specifically hydrogen crossoveracross the PEM from anode to cathode,during fuel cell operations reduces efficiencies and can be the cause ofmembrane degradation effects.Thus, additional gas permeability testing within the temperature and humidity range of operating conditions is required to determine future fuel cell applications for these membranes, which is not addressed in the current study. Specifically, the relationship between gas permeability and both amount and type of PEG incorporation into the membrane would be pertinent to answer if this lower Tg polymer has a negative effect of enhancing gas

crossover. Possible improvements could be partial aromatization, inorganic sol-gel modification, further cross-linking of the membrane to decrease the probability of hydroperoxy or hydroxide radical diffusion, or incorporating a radical trapping material.[38]

4. Conclusion

In summary, the results of the preparation and partial characterization of novel, potentially low cost, high temperature and low humidity PEMs based on poly(1,3-cyclohexadiene) as either homopolymers or as blends and block copolymers with PEG are presented. These materials are considered as limited model systems due to their possible chemical instability. Yet, these materials as membranes can have proton conductivities as high as 18 times that of Nafion even at low relative humidity (20%) and at 120 °C, which is critical for hot and dry fuel cell operation conditions. It is hypothesized that morphologies exhibiting higher connectivity of the hydrophilic domains accounted for their excellent proton conductivities. Simulation and modeling shows a very different PEG distribution between the two membranes and this difference appears to be key in determining the mechanism for higher conductivities. These materials may well degrade in an operating fuel cell because of their aliphatic hydrocarbon character. However, the enhancement of proton conductivity at high temperature and low RH by incorporation of PEG and optimized sulfonation conditions demonstrated here should provide useful insight that will aid in the development of low cost, high temperature PEMs.

ACKNOWLEDGMENT

We gratefully acknowledge the financial support of this research by the U. S. Department of Energy, EERE Program, under Grants # DE-FG36-06GO16037 and DE-FG36-08GO88106, by the U.S. Department of Energy's (DOE) Office of Basic Energy Sciences Program under Grants # DE-FG02-05ER15723, and by the National Science Foundation under Grant # DGE-0801470. A portion of the work at the University of Tennessee was supported by the U. S. National Science Foundation (NSF EPS-1004083, TN Score Thrust 2). Computational work used resources of the National Institute for Computational Sciences (NICS) supported by NSF under agreement number: OCI 07-11134.5. Microscopy research conducted as part of a user proposal at Oak Ridge National Laboratory's Center for Nanophase Materials Sciences (CNMS), which is an Office of Science User Facility.

ABBREVIATIONS

PEM, proton exchange membrane; PCHD, poly(1,3-cyclohexadiene); PCHD-OH; hydroxyl-terminated poly(1,3-cyclohexadiene); xPCHD, cross-linked poly(1,3-cyclohexadiene); xsPCHD, cross-linked, sulfonated poly(1,3-cyclohexadiene); PEG, poly(ethylene glycol); PEI, poly(ethylene imine); Tg, glass transition temperature; RH, relative humidity; THF, tetrahydrofuran; DABCO, 1,4-diazabicyclo-[2.2.2]octane; MePEGBr-2K, Bromide-terminated poly(ethylene glycol) methyl ether with M_n of 2,000 $gmol^{-1}$; $ClSO_3H$, chlorosulfonic acid; S_2Cl_2, sulfur monochloride; BHT, butylated hydroxytoluene; CsI, cesium iodide; RI, refractive index; GPC, Gel permeation chromatography; PDI, polydispersity index; NMR, nuclear magnetic resonance; PTFE, polytetrafluoroethylene; AFM, atomic force microscopy; SEM, scanning electron microscopy; TEM transmission electron microscopy; TGA, thermogravimetric analysis; MD, molecular dynamics; CGMD, coarse-grained molecular dynamics; CRW, confined random

walk; PEG-PEA, poly(ethylene glycol) phenyl ether acrylate; PEGDA, poly(ethylene glycol) diacrylate.

REFERENCES

1. Mathias MF, Makharia R, Gasteiger HA, Conley JJ, Fuller TJ, Gittleman CJ, Kocha SS, Miller DP, Mittelsteadt CK, and Xie T. Electrochem. Soc. Interface 2005;14(3):24-35.
2. Kreuer KD. Solid State Ionics 1997;97(1–4):1-15.
3. Agmon N. Chemical Physics Letters 1995;244(5–6):456-462.
4. Kreuer K-D, Paddison SJ, Spohr E, and Schuster M. Chemical Reviews 2004;104(10):4637-4678.
5. Miyake N, Wainright J, and Savinell R. Journal of the Electrochemical Society 2001;148(8):A898-A904.
6. Adjemian KT, Srinivasan S, Benziger J, and Bocarsly AB. Journal of Power Sources 2002;109(2):356-364.
7. Devanathan R, Venkatnathan A, Rousseau R, Dupuis M, Frigato T, Gu W, and Helms V. The Journal of Physical Chemistry B 2010;114(43):13681-13690.
8. Knox CK and Voth GA. The Journal of Physical Chemistry B 2010;114(9):3205-3218.
9. Esai Selvan M, Calvo-Muñoz E, and Keffer DJ. The Journal of Physical Chemistry B 2011;115(12):3052-3061.
10. Li Q, He R, Jensen JO, and Bjerrum NJ. Chemistry of Materials 2003;15(26):4896-4915.
11. Yeo SC and Eisenberg A. Journal of Applied Polymer Science 1977;21(4):875-898.
12. Thein KYU and Adi E. Mechanical Relaxations in Perfluorosulfonate Ionomer Membranes. Perfluorinated Ionomer Membranes, vol. 180: AMERICAN CHEMICAL SOCIETY, 1982. pp. 79-110.
13. Escoubes M, Pineri M, and Robens E. Thermochimica Acta 1984;82(1):149-160.
14. Bauer F, Denneler S, and Willert-Porada M. Journal of Polymer Science Part B: Polymer Physics 2005;43(7):786-795.
15. Jalani NH and Datta R. Journal of Membrane Science 2005;264(1–2):167-175.
16. Mauritz KA and Moore RB. Chemical Reviews 2004;104(10):4535-4586.
17. Jannasch P. Current Opinion in Colloid & Interface Science 2003;8(1):96-102.
18. Rozière J and Jones DJ. Annual Review of Materials Research 2003;33(1):503-555.
19. Chikashige Y, Chikyu Y, Miyatake K, and Watanabe M. Macromolecules 2005;38(16):7121-7126.
20. Miyatake K, Chikashige Y, and Watanabe M. Macromolecules 2003;36(26):9691-9693.
21. Xing P, Robertson GP, Guiver MD, Mikhailenko SD, and Kaliaguine S. Macromolecules 2004;37(21):7960-7967.
22. Miyatake K, Yasuda T, Hirai M, Nanasawa M, and Watanabe M. Journal of Polymer Science Part A: Polymer Chemistry 2007;45(1):157-163.
23. Miyatake K, Chikashige Y, Higuchi E, and Watanabe M. Journal of the American Chemical Society 2007;129(13):3879-3887.
24. Chen S, Yin Y, Kita H, and Okamoto K-I. Journal of Polymer Science Part A: Polymer Chemistry 2007;45(13):2797-2811.
25. Li N, Zhang S, Liu J, and Zhang F. Macromolecules 2008;41(12):4165-4172.
26. Hlil AR, Matsumura S, and Hay AS. Macromolecules 2008;41(6):1912-1914.
27. Kang S, Zhang C, Xiao G, Yan D, and Sun G. Journal of Membrane Science 2009;334(1–2):91-100.

28. Mader JA and Benicewicz BC. Macromolecules 2010;43(16):6706-6715.
29. Chul Gil S, Chul Kim J, Ahn D, Jang J-S, Kim H, Chul Jung J, Lim S, Jung D-H, and Lee W. Journal of Membrane Science 2012;417–418(0):2-9.
30. Chen S, Chen K, Zhang X, Hara R, Endo N, Higa M, Okamoto K-i, and Wang L. Polymer 2013;54(1):236-245.
31. Li N and Guiver MD. Macromolecules 2014;47(7):2175-2198.
32. Yao B, Yan X, Ding Y, Lu Z, Dong D, Ishida H, Litt M, and Zhu L. Macromolecules 2014;47(3):1039-1045.
33. Ko T, Kim K, Jung B-K, Cha S-H, Kim S-K, and Lee J-C. Macromolecules 2015;48(4):1104-1114.
34. A. Perry K, L. More K, Andrew Payzant E, Meisner RA, Sumpter BG, and Benicewicz BC. Journal of Polymer Science Part B: Polymer Physics 2014;52(1):26-35.
35. Donoso P, Gorecki W, Berthier C, Defendini F, Poinsignon C, and Armand MB. Solid State Ionics 1988;28–30, Part 2(0):969-974.
36. Senadeera GKR, Careem MA, Skaarup S, and West K. Solid State Ionics 1996;85(1–4):37-42.
37. Zhang Z and Xu T. Journal of Materials Chemistry A 2014;2(30):11583-11585.
38. Zhang H and Shen PK. Chemical Reviews 2012;112(5):2780-2832.
39. Mays JW, Deng S, Mauritz KA, Hassan MK, and Gido SP. Materials comprising polydienes and hydrophilic polymers and related methods. vol. US8061533 B2. USA, 2011.
40. Deng S, Hassan MK, Mauritz KA, and Mays JW. Polymer 2015;73:17-24.
41. Borup R, Meyers J, Pivovar B, Kim YS, Mukundan R, Garland N, Myers D, Wilson M, Garzon F, Wood D, Zelenay P, More K, Stroh K, Zawodzinski T, Boncella J, McGrath JE, Inaba M, Miyatake K, Hori M, Ota K, Ogumi Z, Miyata S, Nishikata A, Siroma Z, Uchimoto Y, Yasuda K, Kimijima K-i, and Iwashita N. Chemical Reviews 2007;107(10):3904-3951.
42. Natori I, Imaizumi K, Yamagishi H, and Kazunori M. Journal of Polymer Science Part B: Polymer Physics 1998;36(10):1657-1668.
43. Mango LA and Lenz RW. Die Makromolekulare Chemie 1973;163(1):13-36.
44. Zhong XF and François B. Die Makromolekulare Chemie 1991;192(10):2277-2291.
45. Huang T, Zhou H, Hong K, Simonson JM, and Mays JW. Macromolecular Chemistry and Physics 2008;209(3):308-314.
46. Huang T, Messman JM, and Mays JW. Macromolecules 2008;41(1):266-268.
47. Hong K and Mays JW. Macromolecules 2001;34(4):782-786.
48. Ghosh BD, Lott KF, and Ritchie JE. Chemistry of Materials 2005;17(3):661-669.
49. Johnson BC, Yilgör İ, Tran C, Iqbal M, Wightman JP, Lloyd DR, and McGrath JE. Journal of Polymer Science: Polymer Chemistry Edition 1984;22(3):721-737.
50. Baradie B, Poinsignon C, Sanchez JY, Piffard Y, Vitter G, Bestaoui N, Foscallo D, Denoyelle A, Delabouglise D, and Vaujany M. Journal of Power Sources 1998;74(1):8-16.
51. Blanco JF, Nguyen QT, and Schaetzel P. Journal of Applied Polymer Science 2002;84(13):2461-2473.
52. Gilbert EE. Sulfonation and related reactions. New York: Interscience Publishers, 1965.
53. Thaler WA. Journal of Polymer Science: Polymer Chemistry Edition 1982;20(3):875-896.

54. Mays J and Mauritz KA. Poly(cyclohexadiene)-Based Polymer Electrolyte Membranes for Fuel Cell Applications. University of Tennessee and University of Southern Mississippi, 2011. pp. 1 - 16.
55. Paddison SJ. Annual Review of Materials Research 2003;33(1):289-319.
56. EERE USD-. Hydrogen, fuel cells & infrastructure technologies program multi-year research, development and demonstration plan. . 2007. pp. 332.
57. Esai Selvan M, Keffer DJ, and Cui S. The Journal of Physical Chemistry C 2011;115(38):18835-18846.
58. Yu X, Roy A, Dunn S, Badami AS, Yang J, Good AS, and McGrath JE. Journal of Polymer Science Part A: Polymer Chemistry 2009;47(4):1038-1051.
59. Wang Q, Keffer DJ, and Nicholson DM. The Journal of Chemical Physics 2011;135(21):214903-214901 - 214903-214910.
60. Wang Q, Keffer DJ, Deng S, and Mays J. Polymer 2012;53(7):1517 - 1528.
61. Wang Q, Suraweera NS, Keffer DJ, Deng S, and Mays J. Macromolecules 2012;45(16):6669-6685.
62. Wang Q, Keffer DJ, Deng S, and Mays J. The Journal of Physical Chemistry C 2013;117(10):4901-4912.
63. Wang Q, Keffer DJ, Deng S, and Mays J. Polymer 2013;54(9):2299 - 2307.
64. Humphrey W, Dalke A, and Schulten K. Journal of Molecular Graphics 1996;14(1):33-38.
65. Ennari J, Neelov I, and Sundholm F. Polymer 2001;42(19):8043 - 8050.
66. Nearingburg B and Elias AL. Journal of Membrane Science 2012;389(0):148-154.
67. Williamson DT, Mather B, and Long TE. Journal of Polymer Science Part A: Polymer Chemistry 2003;41:84-93.
68. Natori I and Natori S. Macromolecular Chemistry and Physics 2006;207:1387-1393.
69. Gudipati CS, Greenlief CM, Johnson JA, Prayongpan P, and Wooley KL. Journal of Polymer Science Part A: Polymer Chemistry 2004;42(24):6193-6208.
70. Kim YS and Lee K-S. Polymer Reviews 2015;55(2):330-370.